Weierstraß–Institut
für Angewandte Analysis und Stochastik

im Forschungsverbund Berlin e.V.

Preprint ISSN 0946 – 8633

Thermo-mechanical problems in induction heating of steel

Michael G. Pantelyat [1], Manfred Uhle [2]

submitted: July 3, 2000

[1] Ukrainian National Academy of Sciences
Institute of Problems in Mechanical Engineering
Pozharsky Str. 2/10
UA–61046 Kharkov
Ukraine
E-mail: shulzh@ipmach.kharkov.ua

[2] Weierstrass Institute for Applied Analysis and Stochastics
Mohrenstr. 39
D–10117 Berlin
Germany
E-mail: uhle@wias-berlin.de

Preprint No. 591
Berlin 2000

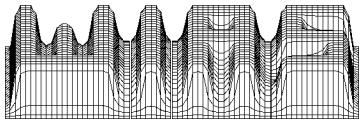

1991 Mathematics Subject Classification. 83C50, 73G25, 58G11.

Key words and phrases. induction heating, Maxwell's equations, heat transfer, mechanical deformations.

Edited by
Weierstraß–Institut für Angewandte Analysis und Stochastik (WIAS)
Mohrenstraße 39
D — 10117 Berlin
Germany

Fax: + 49 30 2044975
E-Mail (X.400): c=de;a=d400-gw;p=WIAS-BERLIN;s=preprint
E-Mail (Internet): preprint@wias-berlin.de
World Wide Web: http://www.wias-berlin.de/

Abstract

We discuss a 3D model that is capable for describing mechanical deformations of steel through induction hardening processes. It consists of a reduced system of Maxwell's equations, the heat transfer equation and a system of equations describing the mechanical state of the steel workpiece.

In a first step the model is applied to simulation of an axisymmetrical induction hardening device, which is a wide-spread industrial equipment. We present numerical results obtained for a steel tube hardening.

1 Introduction

Induction heating plays an important role in the technological process of manufacturing of steel. The induction hardening process of steel is a wide-spread technological operation of modern industry. Figure 1 shows an inductor system of technological device including copper inductor and hardened steel gear-wheel.

In the conducting regions of device under consideration (inductor, gear-wheel) the coupled processes of the alteration of the electromagnetic, thermal and mechanical states take place. Presence of the electromagnetic fields causes thermal and mechanical phenomena. Power losses by Ohm's law alter the temperature distribution and lead to the heating of the workpiece (gear-wheel) and inductor. The temperature gradient alters the mechanical state of the metal structure elements and causes elastic-plastic deformations. In its turn, the non-stationary temperature field influences the electromagnetic processes and electromagnetic field distribution because the conductivity and permeability depend on temperature. Thermal and mechanical properties of metals depend on temperature, too. The above-mentioned complicated effects determine the course and definitive results of technological operations.

Computer simulation of coupled electromagnetic, thermal and mechanical processes taking place during induction heating is an important problem in applied mathematics and engineering.

Numerical modelling and simulation allow to obtain informations for

- optimal shape design of induction coils
- hardening depth, hardness and phase transitions
- choice of technological conditions (frequency of input voltage, duration of heating and cooling).

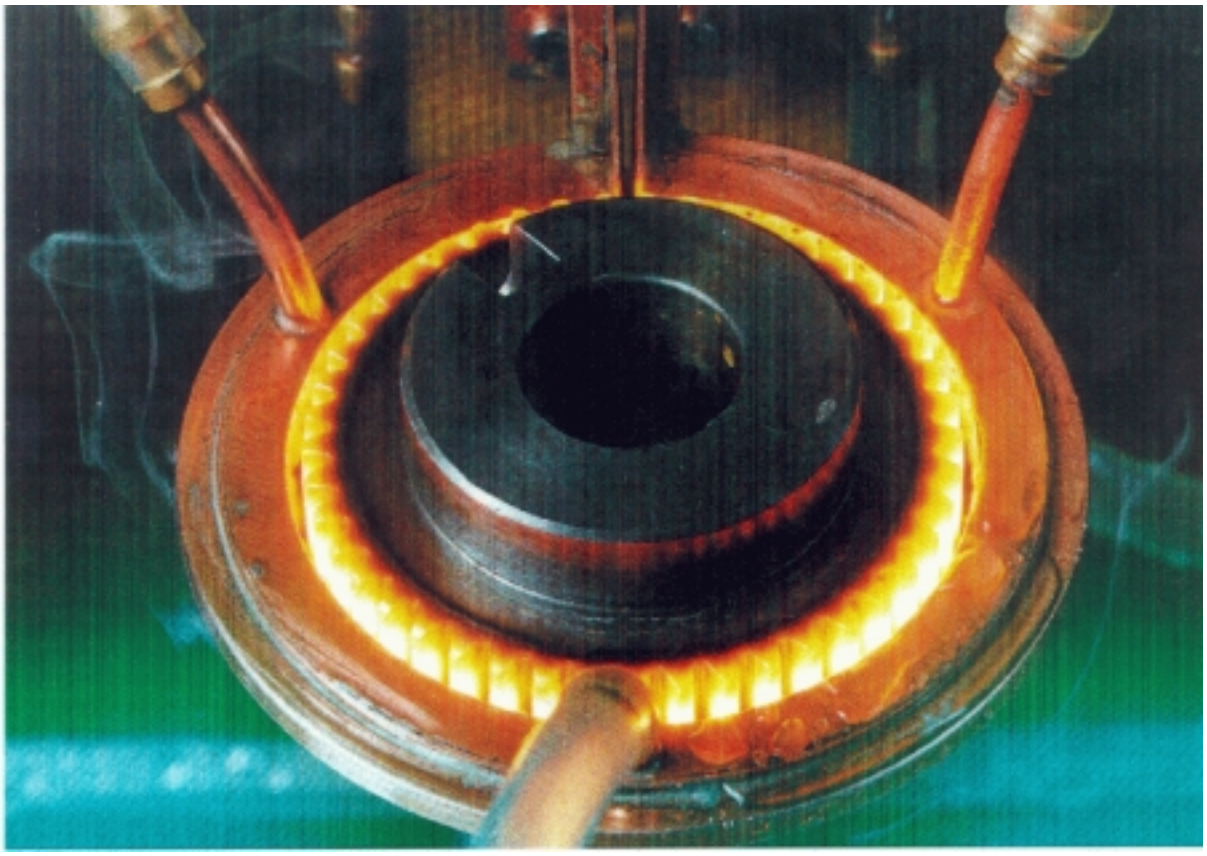

Figure 1: Induction heating at Steremat Elektrowärme GmbH & Co. KG, Berlin

The goal of the paper is to attract attention to necessity of thermo-mechanical problems solution for induction heating devices and to propose mathematical models, numerical formulations and algorithms for such process simulations.

Mathematical models of electromagnetism, temperature distributions and mechanical state of workpieces are presented in the second chapter.

In the first part of the third chapter, our mathematical model is applied to the important case of axisymmetrical geometries of workpieces and inductors.

Numerical simulation results of induction hardening of a metal tube are presented in the second part of the third chapter.

Finally, in the last chapter we conclude the paper with some remarks of further investigations.

2 Process modelling

This chapter presents a general mathematical model of the coupled process of interactions of electromagnetic, temperature and mechanical effects in induction hardening devices (see Figure 2).

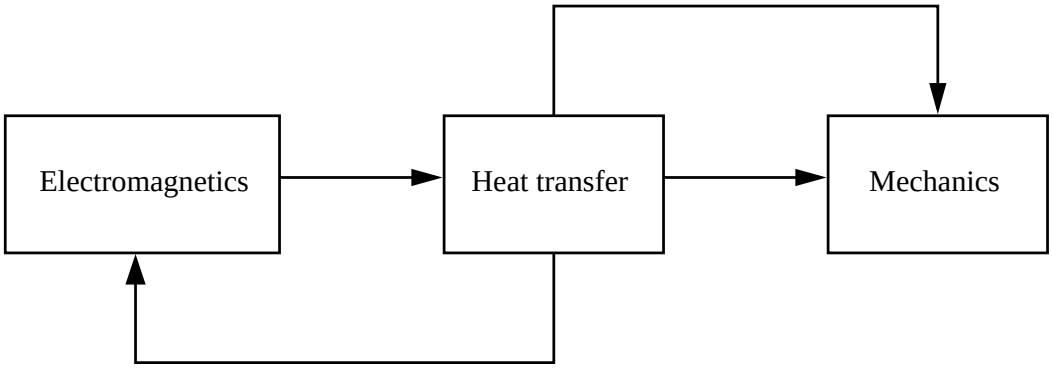

Figure 2: Coupled processes in induction hardening devices

2.1 Modelling of induction heating

For modelling of the induction heating process we have to take into account two different areas (see Figure 3): conducting regions for the workcoil (Ω_{c1}) and for the workpiece (Ω_{c2}) and nonconducting regions for air and for nonferromagnetic materials around the workcoil to reflect the excited magnetic field of the workcoil, shown as Ω_n in Figure 3. The electromagnetic field in the workcoil and in the workpiece is characterized by appreciable skin effect. The boundaries (Γ_B, Γ_H) of the surrounding nonconducting region is described by perfectly conductive or perfectly permeable walls. Therefore, we consider a boundary value problem for the quasistationary Maxwell's equations in a bounded domain:

$$\begin{aligned} rot\vec{H}_c &= \vec{J}_c \\ rot\vec{E}_c &= -\frac{\partial \vec{B}_c}{\partial t} \\ div\vec{B}_c &= 0 \\ \vec{J}_c &= \kappa \vec{E}_c \\ \vec{B}_c &= \mu_c \vec{H}_c \qquad \text{in } \Omega_{c1}, \Omega_{c2}, \end{aligned} \tag{1}$$

and

$$\begin{aligned} rot\vec{H}_n &= \vec{0} \\ div\vec{B}_n &= 0 \\ \vec{B}_n &= \mu_n \vec{H}_n \qquad \text{in } \Omega_n, \end{aligned} \tag{2}$$

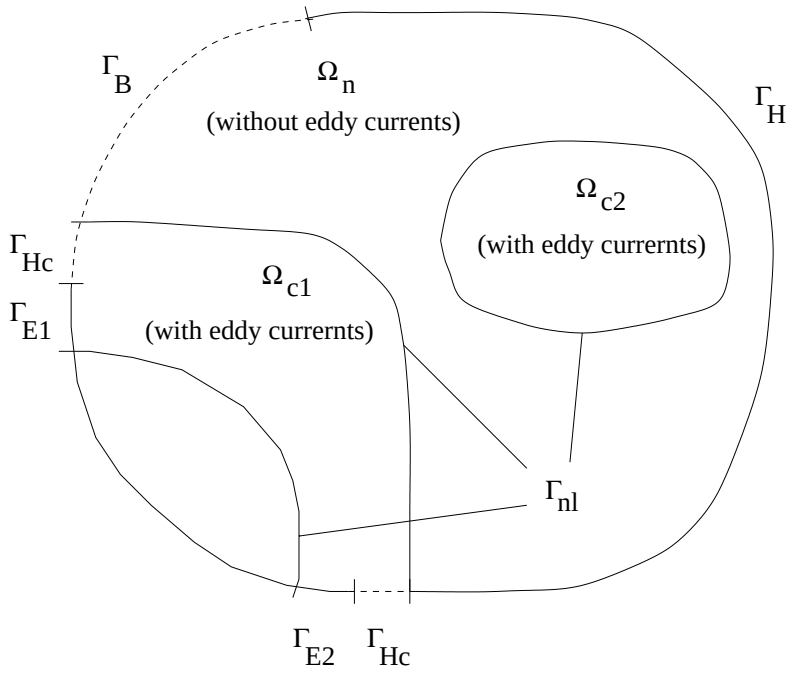

Figure 3: Sketch for modelling the induction heating process

with the boundary conditions

$$\begin{aligned}
\vec{B}_n \cdot \vec{n}_n &= 0 && \text{on } \Gamma_B, \\
\vec{H}_n \times \vec{n}_n &= \vec{0} && \text{on } \Gamma_H, \\
\vec{H}_c \times \vec{n}_c &= \vec{0} && \text{on } \Gamma_{Hc}, \\
\vec{E}_c \times \vec{n}_c &= \vec{0} && \text{on } \Gamma_{E1}, \Gamma_{E2}, \\
\int_{C_{12}} \vec{E}_c \cdot d\vec{r} &= U && \text{on } \Gamma_{E1}, \Gamma_{E2},
\end{aligned} \tag{3}$$

the interface conditions on Γ_{nc}

$$\begin{aligned}
\vec{B}_c \cdot \vec{n}_c + \vec{B}_n \cdot \vec{n}_n &= 0, \\
\vec{H}_c \times \vec{n}_c + \vec{H}_n \times \vec{n}_n &= \vec{0}
\end{aligned} \tag{4}$$

and suitable initial conditions for $\vec{B}_c(\cdot, t_0)$ and $\vec{B}_n(\cdot, t_0)$.

In the literature several finite element formulations for the calculation of three dimensional eddy current problems have been considered e.g. [1], [2]. We introduce a magnetic vector potential $\vec{A}$ and a scalar potential Φ by

$$\begin{aligned}
\vec{B} &= rot\vec{A} \\
\vec{E} &= -\frac{\partial \vec{A}}{\partial t} - grad\Phi
\end{aligned}$$

and use the $\vec{A}, \Phi - \vec{A}$ formulation [1] to describe general geometrical situations. Now, we rewrite equations (1), (2) and enforce the uniqueness of the vector potential by Coulomb gauging [1] in the following way:

$$
\begin{aligned}
rot\frac{l}{\mu_c}rot\vec{A}_c \;-\; grad\frac{1}{\mu_c}div\vec{A}_c \;+\; \kappa\frac{\partial\vec{A}_c}{\partial t} \;+\; \kappa grad\Phi \;&=\; \vec{0} \\
div\left(-\kappa\frac{\partial\vec{A}_c}{\partial t} - \kappa grad\Phi\right) \;&=\; 0 \qquad\qquad \text{in } \Omega_{c1}, \Omega_{c2}, \\
rot\frac{1}{\mu_n}rot\vec{A}_n - grad\frac{1}{\mu_n}div\vec{A}_n \;&=\; \vec{0} \qquad\qquad \text{in } \Omega_n
\end{aligned}
$$

with initial values for $\vec{A}_c(\cdot, t_0)$ and $\vec{A}_n(\cdot, t_0)$. Rewriting boundary conditions (3) to

$$
\begin{aligned}
\vec{n}_n \times \vec{A}_n \;&=\; \vec{0} \qquad\qquad \text{on } \Gamma_B, \\
\frac{1}{\mu_n}div\vec{A}_n \;&=\; 0 \qquad\qquad \text{on } \Gamma_B, \\
(\frac{1}{\mu_n}rot\vec{A}_n) \times \vec{n}_n \;&=\; \vec{0} \qquad\qquad \text{on } \Gamma_H, \\
\vec{A}_n \cdot \vec{n}_n \;&=\; 0 \qquad\qquad \text{on } \Gamma_H, \\
(\frac{1}{\mu_c}rot\vec{A}_c) \times \vec{n}_c \;&=\; \vec{0} \qquad\qquad \text{on } \Gamma_{Hc}, \\
\vec{A}_c \cdot \vec{n}_c \;&=\; 0 \qquad\qquad \text{on } \Gamma_{Hc}, \\
\vec{n}_c \cdot (\kappa\frac{\partial\vec{A}}{\partial t} \;+\; \kappa grad\Phi) \;&=\; 0 \qquad\qquad \text{on } \Gamma_{Hc}, \\
\vec{n}_c \times \vec{A}_c \;&=\; \vec{0} \qquad\qquad \text{on } \Gamma_{E1}, \Gamma_{E2}, \\
\frac{1}{\mu_c}div\vec{A}_c \;&=\; 0 \qquad\qquad \text{on } \Gamma_{E1}, \Gamma_{E2}, \\
\Phi|_{\Gamma_{E1}} \;&=\; U \qquad\qquad \text{on } \Gamma_{E1}, \Gamma_{E2}, \\
\Phi|_{\Gamma_{E2}} \;&=\; 0 \qquad\qquad \text{on } \Gamma_{E1}, \Gamma_{E2}
\end{aligned}
$$

and interface conditions (4) on Γ_{nc} to

$$
\begin{aligned}
(rot\vec{A}_c) \cdot \vec{n}_c \;+\; (rot\vec{A}_n) \cdot \vec{n}_n \;&=\; 0 \\
(\frac{1}{\mu_c}rot\vec{A}_c) \times \vec{n}_c \;+\; (\frac{1}{\mu_n}rot\vec{A}_n) \times \vec{n}_n \;&=\; \vec{0} \\
\vec{n}_c \cdot (\kappa\frac{\partial\vec{A}}{\partial t} \;+\; \kappa grad\Phi) \;&=\; 0 \\
\vec{n}_n \cdot \frac{1}{\mu_n}div\vec{A}_n + \vec{n}_c \cdot \frac{1}{\mu_c}div\vec{A}_c \;&=\; 0
\end{aligned}
$$

one takes notice of additional conditions enforcing the Coulomb gauge on the vector potential.

Owing to the Ohm's law, the eddy currents induced in the workpiece act as a heat source, which can be described by

$$q(\theta) = \kappa(\theta)\left|\vec{E}\right|^2. \tag{5}$$

2.2 Modelling of temperature distributions in steel

Neglecting mechanical effects and using Fourier's law of heat conduction, we consider the following heat transfer equation:

$$\rho(\theta)c(\theta)\frac{\partial\theta}{\partial t} \; - \; \nabla\cdot\Big(\beta(\theta)\nabla\theta\Big) \;\; = \;\; q(\theta), \qquad \text{in } \Omega_{c_2}\times(0,T). \tag{6}$$

Here, Ω_{c_2} is the workpiece and ρ, c, β denote density, specific heat at constant pressure and heat conductivity, respectively. The term $q(\theta)$ describes the induction heat source (5).

We consider a Newton-type boundary condition

$$-\beta(\theta)\frac{\partial\theta}{\partial\nu} = \gamma(x,t)(\theta-\theta_\Gamma) \qquad \text{in } \partial\Omega_{c_2}\times(0,T),$$

where γ denotes the heat exchange coefficient. The initial condition is set to

$$\theta(\cdot,0) = \theta_0 \qquad \text{in} \quad \Omega_{c_2}.$$

2.3 Modelling of elastic-plastic deformations

The elastic-plastic mechanical state of the workpiece is described by the following system of equations [3] [4]

$$0 \;\; = \;\; \frac{\partial\sigma_{ij}}{\partial x_i} + F_i \tag{7}$$

$$\varepsilon_{ij} \;\; = \;\; 0.5\,(\frac{\partial u_i}{\partial x_j} + \frac{\partial u_j}{\partial x_i}) \tag{8}$$

$$\sigma_{ij} \;\; = \;\; 2G(\varepsilon_{ij} + \frac{\nu}{1-2\nu}\,\delta_{ij}e), \tag{9}$$

where $i = 1,2,3$ and $j = 1,2,3$ are numbers of coordinate axes.

System of equilibrium equations (7) describes correlations between mechanical stress tensor

$$\sigma = \begin{pmatrix} \sigma_{11} & \sigma_{12} & \sigma_{13} \\ \sigma_{21} & \sigma_{22} & \sigma_{23} \\ \sigma_{31} & \sigma_{32} & \sigma_{33} \end{pmatrix} \tag{10}$$

and given forces components F_i.

Kinematic equations (8) represent correlations between strain tensor

$$\varepsilon = \begin{pmatrix} \varepsilon_{11} & \varepsilon_{12} & \varepsilon_{13} \\ \varepsilon_{21} & \varepsilon_{22} & \varepsilon_{23} \\ \varepsilon_{31} & \varepsilon_{32} & \varepsilon_{33} \end{pmatrix} \tag{11}$$

and mechanical displacement components u_i.

Constitutive equations (9) are correlations between mechanical stresses σ_{ij} and strains ε_{ij}, where δ_{ij} is the Kronecker's delta function, ν is Poisson's number, e represents the main diagonal of matrix (11) and G describes the dislocation modulus by

$$G = \frac{E}{2(1+\nu)}, \tag{12}$$

where E is the modulus of elasticity.

In order to simulate mechanical state of workpieces during induction heating we take into account elastic, plastic and thermal deformations. Therefore, we present strain tensor ε_{ij} as a sum of elastic ε^e_{ij}, plastic ε^p_{ij} and thermal ε^θ_{ij} strain components:

$$\varepsilon_{ij} = \varepsilon^e_{ij} + \varepsilon^p_{ij} + \varepsilon^\theta_{ij}. \tag{13}$$

We can write the following expressions for different components of the strain tensor (13). The first component is elastic strains

$$\varepsilon^e_{ij} \;=\; \frac{1}{E}[(1 \;+\; \nu)\;\sigma_{ij} \;-\; \delta_{ij}\;\nu\;s], \tag{14}$$

where s describes the main diagonal of tensor σ, see (10). It is the another form of the constitutive equations (9).

The second component of (10) is thermal strains [3] [4]

$$\varepsilon^\theta_{ij} = \alpha\Delta\theta\delta_{ij}, \tag{15}$$

where α is the coefficient of linear temperature expansion and $\Delta\theta$ is the difference of temperature.

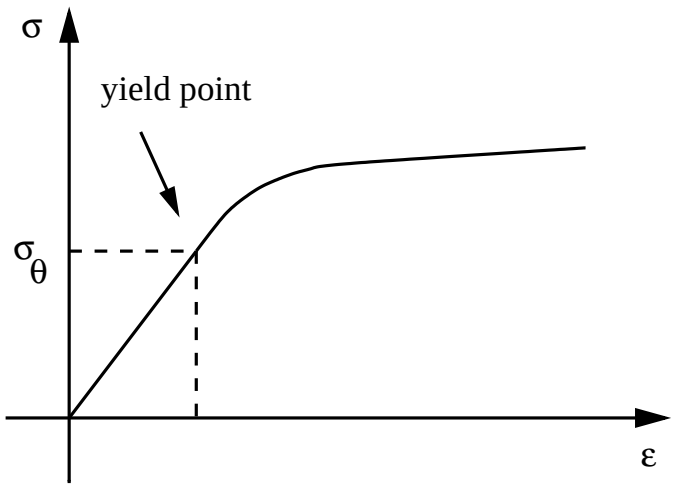

Figure 4: Elastic-plastic diagram of the steel

The last component in (13) denotes the plastic strains [5]. We can use the incremental theory of plasticity taking into account correlations between increments of plastic strains $\Delta\varepsilon_{ij}^{p}$ and increments of mechanical stresses $\Delta\sigma_{ij}$:

$$\Delta\varepsilon_{ij}^{p} = \left(\frac{3}{2\sigma_i}\right)^2 \left(\frac{1}{E_k} - \frac{1}{E}\right) S_{ij} S_{km} \Delta\sigma_{km} + \left(\frac{3}{2\sigma_i}\right) \left(\frac{1}{E_k} - \frac{1}{E}\right) (\sigma_i - \sigma_\theta)\delta_{ij}\Delta\sigma_{mm}, \quad (16)$$

where σ_i denotes the intensity of stresses in the form of

$$\sigma_i = \frac{1}{3}\sqrt{(\sigma_{11} - \sigma_{22})^2 + (\sigma_{22} - \sigma_{33})^2 + (\sigma_{11} - \sigma_{33})^2 + 6(\sigma_{12}^2 + \sigma_{23}^2 + \sigma_{13}^2)}, \quad (17)$$

σ_θ is the yield point (refer to Figure 4), E_k is the tangential modulus from the strain diagram, S_{ij} denotes the stress deviator by

$$S_{ij} = \sigma_{ij} - \frac{1}{3}\sigma_{ij}\delta_{ij}. \quad (18)$$

In order to use the above-mentioned incremental theory of plasticity we present the plastic strain tensor ε_{ij}^{p} and stress tensor σ_{ij} in the following form:

$$\varepsilon_{ij}^{p} = \overline{\varepsilon}_{ij}^{p} + \Delta\varepsilon_{ij}^{p}, \quad (19)$$

$$\sigma_{ij} = \overline{\sigma}_{ij} + \Delta\sigma_{ij}, \quad (20)$$

where $\overline{\varepsilon}_{ij}^{p}$ and $\overline{\sigma}_{ij}$ are the known plastic strain and stress tensors values obtained from previous time step.

3 Simulation of axisymmetrical induction heating device

3.1 Axisymmetrical formulation

We consider axisymmetrical positioning of the impulse inductive device depicted schematically in Figure 5. The equation of the impulse electromagnetic field in the case of axisymmetrical problems can be written as follows [6], [9]:

$$\kappa(\theta)\frac{\partial A}{\partial t} = \frac{\partial}{\partial r}\left(\frac{1}{\mu(H,\theta)}\frac{1}{r}\frac{\partial(rA)}{\partial r}\right) + \frac{\partial}{\partial z}\left(\frac{1}{\mu(H,\theta)}\frac{\partial A}{\partial z}\right) + J_o, \tag{21}$$

where A is the magnetic vector potential, $\kappa(\theta)$ is the temperature-dependent conductivity of the material, θ is the temperature, $\mu(H,\theta)$ is the permeability depending on the magnetic field strength H and on the temperature θ, and J_o is the given source current density.

The thermal field is described by the Fourier's equation [6], [9]

$$\rho c(\theta)\frac{\partial \theta}{\partial t} = \frac{1}{r}\frac{\partial}{\partial r}\left(r\beta(\theta)\frac{\partial \theta}{\partial r}\right) + \frac{\partial}{\partial z}\left(\beta(\theta)\frac{\partial \theta}{\partial z}\right) + q(\theta), \tag{22}$$

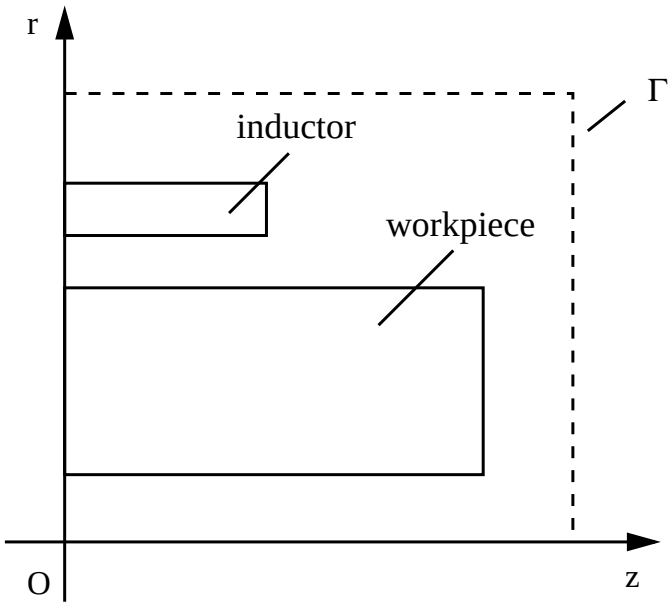

Figure 5: Sketch of an axisymmetrical induction device

where $c(\theta)$ is the temperature-dependent specific heat of the material, ρ is the mass density, $\beta(\theta)$ is the temperature-dependent thermal conductivity, and q is the electric power density.

The static axisymmetrical elastic-plastic mechanical state of metal regions (coil, work-piece) can be calculated solving the following system of equations [4], [6]:

$$\begin{aligned}
&\frac{\partial \sigma_{rr}}{\partial r} + \frac{\partial \tau_{rz}}{\partial z} - \frac{\sigma_{rr} - \sigma_{\theta\theta}}{r} + F_r = 0, \\
&\frac{\partial \tau_{rz}}{\partial r} + \frac{\partial \sigma_{zz}}{\partial z} + \frac{\tau_{rz}}{z} + F_z = 0, \\
&\varepsilon_{rr} = \frac{\partial u_r}{\partial r}, \quad \varepsilon_{zz} = \frac{\partial u_z}{\partial z}, \quad \varepsilon_{\theta\theta} = \frac{u_r}{r}, \\
&\gamma_{rz} = \frac{\partial u_r}{\partial z} + \frac{\partial u_z}{\partial r},
\end{aligned} \tag{23}$$

where σ_{rr}, σ_{zz}, $\sigma_{\theta\theta}$, τ_{rz} are the radial, axial, azimuthal and tangential mechanical stresses, respectively, ε_{rr}, ε_{zz}, $\varepsilon_{\theta\theta}$, γ_{rz} are the radial, axial, azimuthal and tangential mechanical strains, respectively, u_r, u_z are the radial and axial mechanical displacements, and F_r, F_z are the given radial and axial forces.

The detailed finite element formulations for equations (21), (22) and system (23) have been presented in [6], [9]. The feature of impulse electromagnetic, transient thermal and static mechanical processes does not allow the use of the usual method, which consists in dividing the duration of process into a series of time steps, and in the simultaneous [7] or successive [8] solution of the electromagnetic and thermo-mechanical problems for every time step. The point is that such a time-stepping algorithm requires huge computational expenses, especially in the case of multi-impulse processes. Therefore, in order to carry out a fast and accurate simulation of the mentioned processes the following indirect coupling algorithm is proposed:

- We divide the first pulse into a series of small time steps Δt_1 and solve the electromagnetic problem (21) for all steps in succession. As a result we obtain the space distribution of the magnetic vector potential A, current density $J = J_o - \kappa \dfrac{\partial A}{\partial t}$ and the electric power density $q(r,z,t) = \dfrac{J^2}{\kappa}$ at every time step.

- The obtained values of the heat sources $q(r,z,t)$ are averaged in time for the first pulse:

$$Q(r,z) = \frac{1}{T_1} \int_0^{T_1} q(r,z,t)\, dt, \tag{24}$$

  where T_1 is the duration of the pulse or the sum duration of the pulse and the pause between two successive impulses.

- We divide the duration of the process into a series of large time steps $\Delta t_2 \gg \Delta t_1$ and solve the thermo-mechanical problems (22), (23) with constant in time space distribution of the heat sources (24). Like that, we extend the calculated heat sources to a number of the next impulses or to the whole duration of the process.
- We use the obtained temperature distribution in order to calculate new values of temperature-dependent electric, thermal and mechanical material properties.
- Using obtained material properties we repeat the electromagnetic field simulation, calculate and average the electric power density, and so on. New problems solution with new material properties is carried out after the sum duration of a number of the next pulses and pauses. The increase of the number of solutions raises the accuracy of the computation and, of course, computational expenses.

Solving the transient eddy current problem (21) for soft ferromagnetic materials we use the internal iterative process proposed by the first author [10]. The use of very large time steps Δt_2 for thermo-mechanical problem allows to reduce essentially computational expenses and to obtain reliable and accurate numerical results.

3.2 Numerical results

We solved an axisymmetrical problem of practical interest concerning magneto-thermo-mechanical behaviour of heated steel [6].

The goal of investigation is to determine and recommend technological and exploitational conditions of inductive heating from thermal and mechanical points of view (maximal temperatures, mechanical stresses and displacements etc.).

Figure 5 shows the positioning of the inductive equipment including copper inductor, heated steel tube and air regions. The amplitude of the current equals 111.6 kA, frequency is 8 kHz, capacitor generator depicted in Figure 6 generates 1000 impulses per second, duration of heating is 9 s, material constants have been presented in [6].

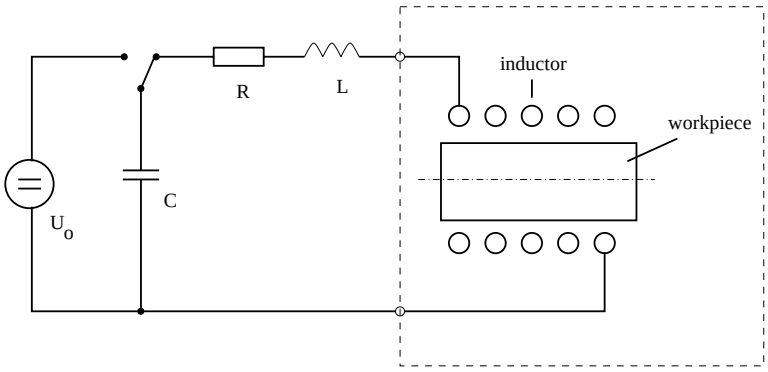

Figure 6: Principle sketch of an impulse induction technological device

Equation (21) has been solved by using the following boundary conditions (see Fig. 5):

- on the axis of symmetry (z=0) : $\dfrac{\partial A}{\partial z} = 0$;
- the axis of anti-symmetry (r=0) : A = 0;
- on the distant bound Γ : the boundary condition of the third kind using the known analytical solution for magnetic field of the solenoid [9].

The thermal field has been simulated by using boundary conditions of the third kind [9] corresponding to air quenching (the heat transfer coefficient $\alpha = 50\ Wm^{-2}K^{-1}$, the air temperature is 20^o C). Besides, we have taken into account the thermal radiation in accordance with Stefan-Boltzmann's law [9] (emissivity $\varepsilon = 0.8$).

The static mechanical problem (23) has been solved by kinematic boundary condition $u_z = 0$ on the axis of symmetry (z=0).

The results have been obtained using multiple solution of the problems (at the initial temperature 20^oC and when duration of heating equals 0.9 s, 2 s, 5 s, 7 s, and 9 s). Time steps Δt_1 (see above) for electromagnetic problem (21) have been determined by means of dividing every peak of the pulsed current (see Figure 7) on 40 equal time intervals. Time steps $\Delta t_2 \gg \Delta t_1$ for the thermo-mechanical problem (2), (3) have been determined by means of dividing every time intervals between two successive solutions on 20 equal intervals.

As result Figure 8 shows the space distribution of the magnetic vector potential. Temperature distribution and deformated state of the workpiece (duration of heating is 9s) are presented in Figure 9 on page 14 and the state of stress of heated tube is shown in Figure 10. The surface of the workpiece is heated to 1100^oC. There are compressing mechanical stresses on the external surface and stretching stresses on the internal one.

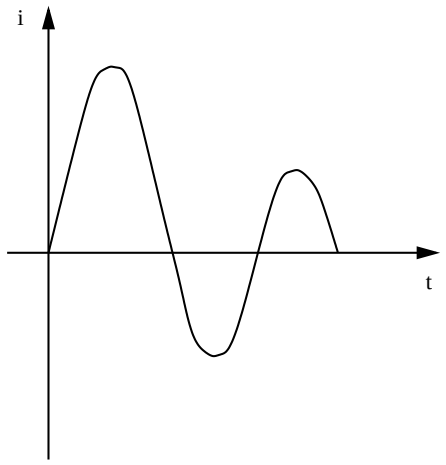

Figure 7: Pulsed current in the inductor

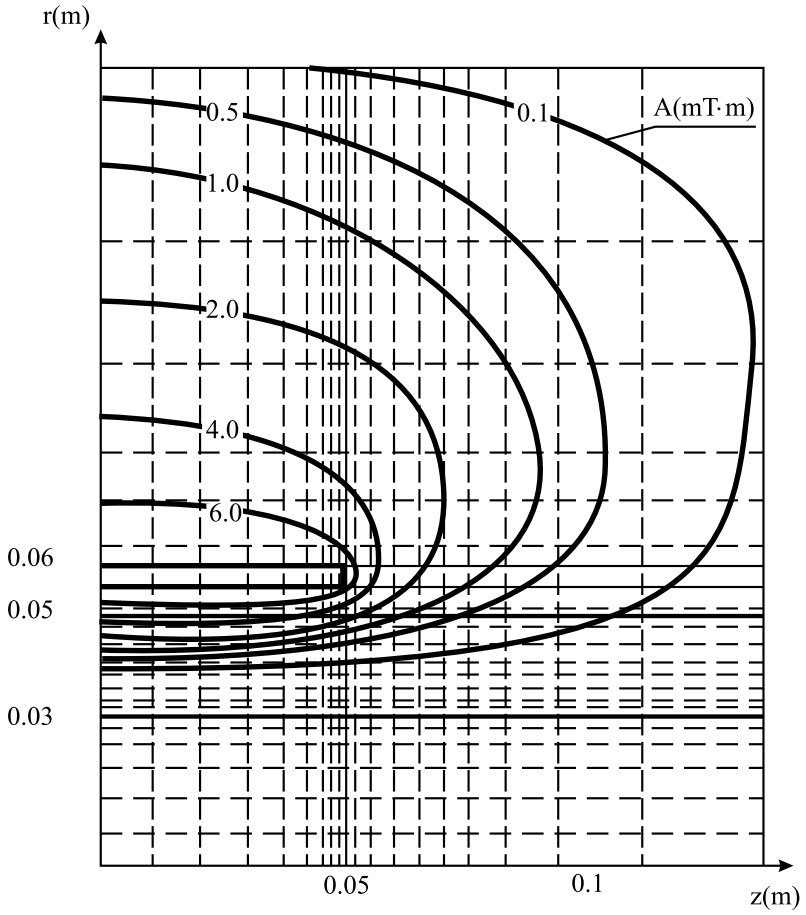

Figure 8: Positioning of induction device and distribution of the magnetic vector potential at $t = 37.5\mu s$

The obtained results testify about the correct choice of the inductive heating technological conditions. The surface temperature and the velocity of the heating correspond to the conditions required for the steel under consideration. Besides, we can see the small level of mechanical stresses and displacements (the maximum values of radial and axial displacements equal 0.5 mm, approximately).

4 Conclusion

We have proposed a general three dimensional mathematical model, numerical formulation and algorithm for simulation of coupled magneto-thermo-mechanical processes in induction heating devices.

Such simulations allow to obtain precise information about thermo-mechanical state of heated workpiece and to determine important technological conditions of induction heating (frequency of input voltage, duration of heating and cooling, etc.).

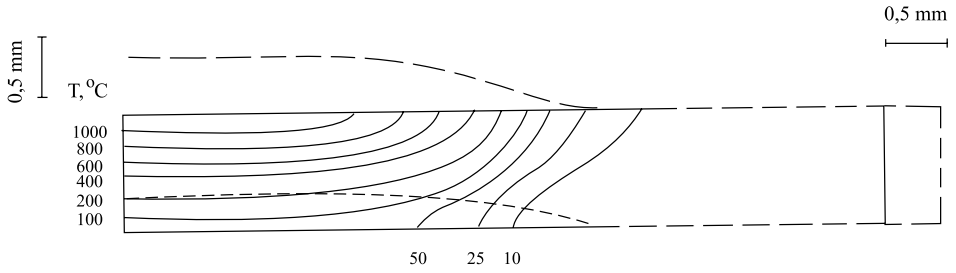

Figure 9: Temperature distribution and deformated state of the workpiece

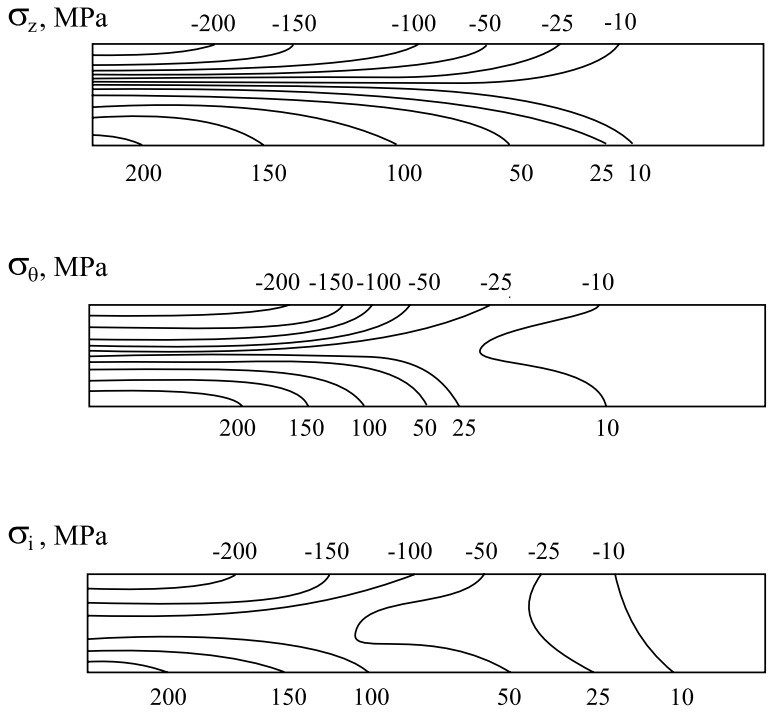

Figure 10: State of stress of the workpiece

As a numerical example we have used an axisymmetrical impulse induction heating device for steel tubes hardening. Axisymmetrical formulation for coupled magneto-thermo-mechanical simulation has been presented. Obtained numerical results testify about a correct choice of technological conditions of induction heating.

On our opinion the main direction of future investigations is numerical realization of proposed general three dimensional models and algorithms in order to simulate industrial induction devices with complicated geometry of workpieces and inductor coils.

References

[1] O. Biro and K.Preis, *On the use of the magnetic vector potentialin the finite element analysis of 3D eddy currents*, IEEE Trans. Magn. vol. MAG-25(1989) 7, pp. 3145–3159.

[2] O. Biro, K.Preis and K. R. Richter, *Various FEM formulations for the caculations of transient 3D eddy currents in nonlinear media*, IEEE Trans. Magn. vol. MAG-31(1995) 5, pp. 1307–1312.

[3] H.G. Hahn, *Elastizitätstheorie*, Stuttgart: B.G. Teubner, 1985.

[4] S. Timoshenko and J.N. Goodier, *Theory of Elasticity*, New York: Mc-Graw Hill, 1951.

[5] J. Zgraja and M.G. Pantelyat, *Inductive heating of large steel disks: coupled electromagnetic, thermal and mechanical simulation*, International Journal of Applied Electromagnetics and Mechanics, vol. 10, pp.303-313, 1999.

[6] M. G. Pantelyat, *Coupled electromagnetic, thermal and elastic-plastic simulation of multi-impulse inductive heating*, Int. J. Appl. Electromagnetics and Mechanics, vol. 9, pp. 11-24, 1998.

[7] M. Féliachi and G. Develey, *Magneto-thermal behavior finite element alalysis for ferromagnetic materials in induction heating devices*, IEEE Trans. Magn., vol. 27, Pt. II, pp. 5235-5237, Nov. 1991.

[8] Ph. Massé, B. Morel, and Th. Bréville, *A finite element prediction correction scheme for magneto-thermal coupled problem during Curie transition*, IEEE Trans. Magn., vol. 21, Sept. 1985.

[9] P. P. Gontarowsky and M. G. Pantelyat, *Application of the finite element method to coupled eddy current, thermal and mechanical problems,* Proc. 6th Int. IGTE Symposium on Numerical Field Calculation in Electrical Engineering, Graz, pp. 300-308, 1994.

[10] M. G. Pantelyat, *Numerical analysis of impulse electromagnetic fields in soft ferromagnetic materials,* Int. J. Appl. Electromagnetics and Mechanics, vol. 10, pp. 185-192, 1999.